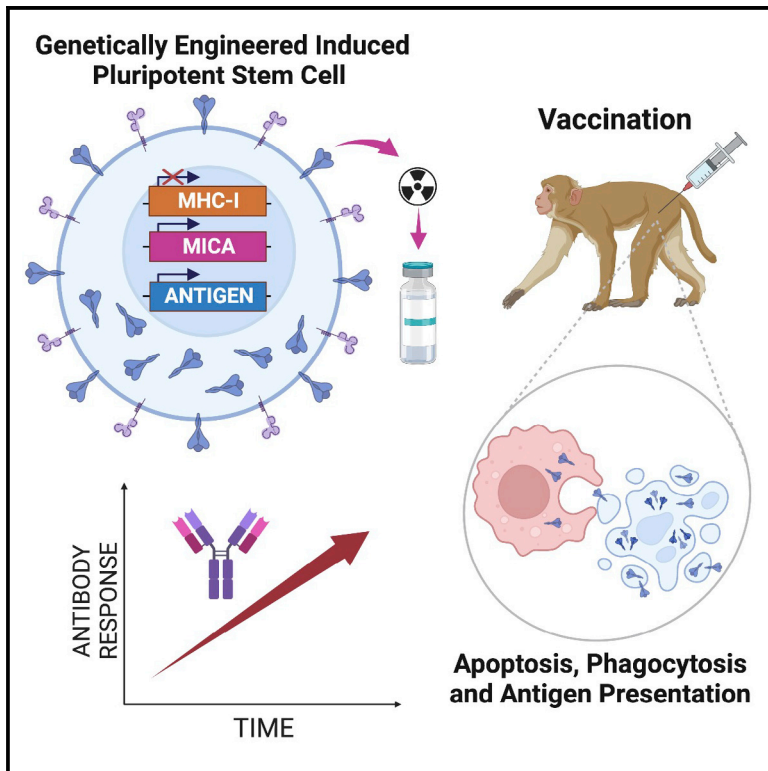**Article**

A genetically engineered, stem-cell-derived cellular vaccine

Graphical abstract

Authors

Amanda Cooper, Adam Sidaway,
Abishek Chandrashekar, ...,
Modassir Choudhry, Tom Henley,
Dan H. Barouch

Correspondence

tom@intimabioscience.com (T.H.),
dbarouch@bidmc.harvard.edu (D.H.B.)

In brief

Cooper et al. describe a genetically
engineered cellular vaccine designed to
recapitulate natural physiological
immunity induced upon viral infection of
host cells. The scalable and poly-
antigenic vaccine technology can induce
robust and durable antibody responses
to SARS-CoV-2 virus as a representative
model of viral infection.

Highlights

- A universal vaccine cell genetically engineered to mimic natural viral immunity

- SARS-CoV-2 spike vaccine cells induce robust neutralizing antibodies upon immunization

- Reduced SARS-CoV-2 RNA in lungs of vaccinated animals challenged with a viral variant

CelPress

Article

A genetically engineered, stem-cell-derived cellular vaccine

Amanda Cooper,[2] Adam Sidaway,[2] Abishek Chandrashekar,[3] Elizabeth Latta,[2] Krishnendu Chakraborty,[2] Jingyou Yu,[3] Katherine McMahan,[3] Victoria Giffin,[3] Cordelia Manickam,[3] Kyle Kroll,[3] Matthew Mosher,[3] R. Keith Reeves,[3] Rihab Gam,[2] Elisa Arthofer,[2] Modassir Choudhry,[1,2] Tom Henley,[1,2,*] and Dan H. Barouch[3,4,5,*]

[1]Praesidium Bioscience, Inc., New York, NY, USA
[2]Intima Bioscience, Inc., New York, NY, USA
[3]Center for Virology and Vaccine Research, Beth Israel Deaconess Medical Center, Harvard Medical School, Boston, MA, USA
[4]Ragon Institute of Massachusetts General Hospital, Massachusetts Institute of Technology, and Harvard University, Cambridge, MA, USA
[5]Lead contact
*Correspondence: tom@intimabioscience.com (T.H.), dbarouch@bidmc.harvard.edu (D.H.B.)
https://doi.org/10.1016/j.xcrm.2022.100843

SUMMARY

Despite rapid clinical translation of COVID-19 vaccines in response to the global pandemic, an opportunity remains for vaccine technology innovation to address current limitations and meet challenges of inevitable future pandemics. We describe a universal vaccine cell (UVC) genetically engineered to mimic natural physiological immunity induced upon viral infection of host cells. Cells engineered to express the severe acute respiratory syndrome coronavirus 2 (SARS-CoV-2) spike as a representative viral antigen induce robust neutralizing antibodies in immunized non-human primates. Similar titers generated in this established non-human primate (NHP) model have translated into protective human neutralizing antibody levels in SARS-CoV-2-vaccinated individuals. Animals vaccinated with ancestral spike antigens and subsequently challenged with SARS-CoV-2 Delta variant in a heterologous challenge have an approximately 3 log decrease in viral subgenomic RNA in the lungs. This cellular vaccine is designed as a scalable cell line with a modular poly-antigenic payload, allowing for rapid, large-scale clinical manufacturing and use in an evolving viral variant environment.

INTRODUCTION

The COVID-19 pandemic has demonstrated the urgent need for new innovations in vaccinology to enable the rapid development of novel vaccines against emerging viral variants that engender robust and long-lasting immune protection. The unprecedented success of both mRNA and adenoviral vaccines has established the capability of a rapid global vaccination program.[1–3] However, the waning antibody responses seen with these emergency-use-authorized vaccine technologies, and the need for vaccine boosters, has highlighted the requirement for further improvements in vaccine approaches to drive higher, longer-lasting protective immunity.[4–9] The newly emerging viral variants of SARS-CoV-2, and the evident reduced efficacy of the existing vaccines to protect against transmissible and symptomatic infection of these variants, also highlights the need for vaccines that can ideally deliver multiple variant antigens (polyvalency) and be rapidly manufactured at scale as soon as new viral variants are discovered.[10–13]

Theoretically, an ideal vaccine technology would have four core attributes, namely robust immunity, self-adjuvancy, polyvalency, and scalability. Immunity is self-evident and speaks to the requirement of generating robust humoral neutralizing antibody and ideally T cell responses that are durable. Self-adjuvancy, or conversely the absence of the need for exogenous excipients to elicit a robust immune response, may prove to be a meaningful innovation in that the immune side effects of current vaccines may be mediated by the non-target-antigen-specific adjuncts.[14] Thirdly, polyvalency, or the ability to protect against multiple immunodominant epitopes, is a core feature of overlapping and orthogonal mechanisms of protection.[15,16] Lastly, scalability or the ability to deliver preventative doses of vaccines in an economic, large-scale, and clinically relevant fashion in both the developed and developing worlds is a *sine qua non* of any human vaccine.

Current mRNA-, protein-, and viral-vector-based vaccines have certain limitations, such as their requirement for excipient adjuvants to activate the recipient immune system or to deliver the viral antigenic payload.[17,18] These include the artificial lipid nanoparticles delivering the mRNA, or MF59, AS03, Alum, ISCOMATRIX, and Matrix-M chemical emulsions, for example, or the adenoviral protein antigens themselves that stimulate innate immune cell activation.[18–24] Adjuvants are required to increase the effectiveness of vaccines, and their use can cause side effects including local reactions (redness, swelling, and
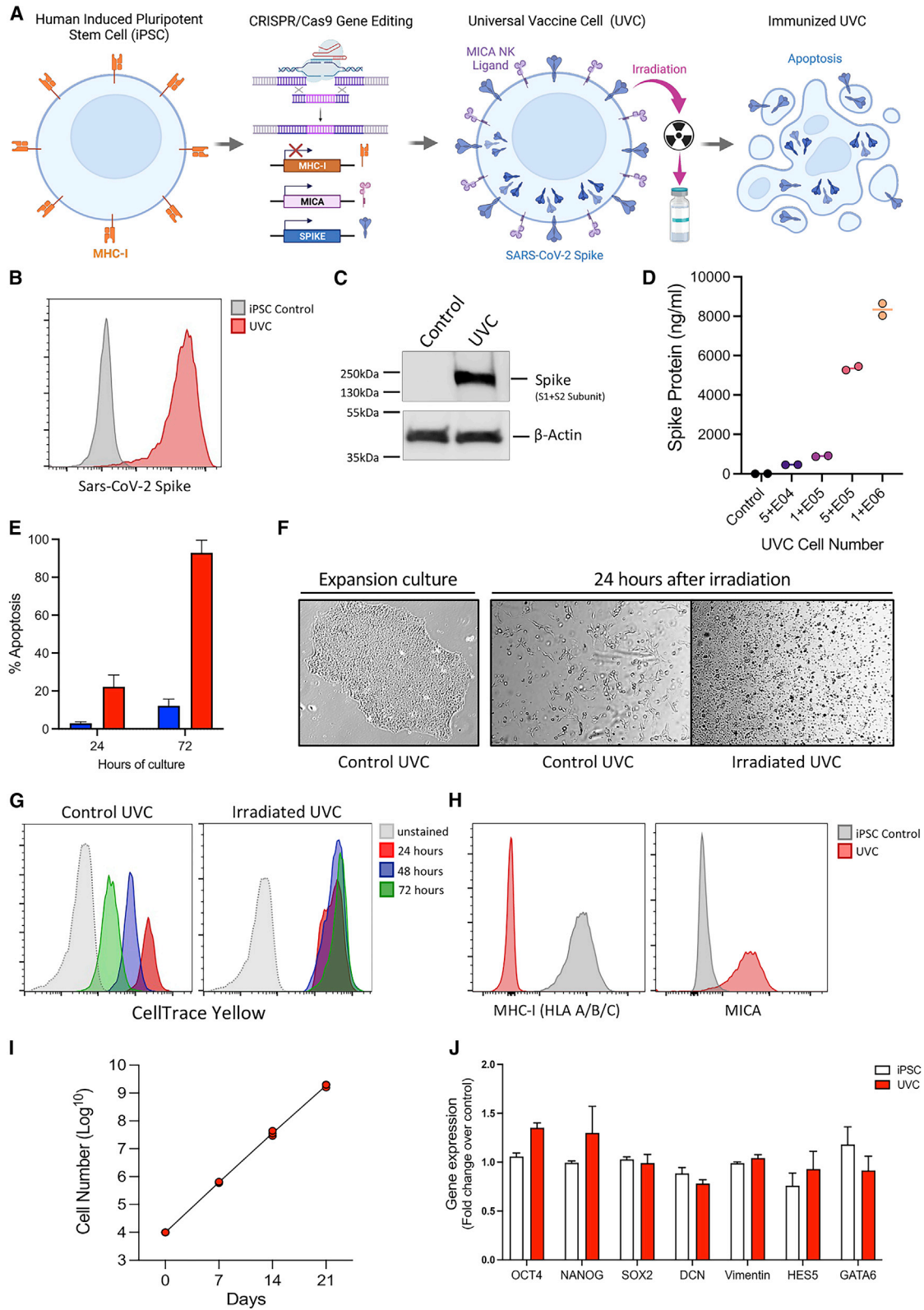
pain at the injection site) and systemic reactions (fever, chills, and body aches).[25–27]

The size constraint of the adenoviral vector genome, and the limited length of stable mRNA that can be produced and packaged into nanoparticles, restricts the number and size of nucleic-acid-encoded antigens and epitopes that can be delivered in these vaccines.[28] Thus, these vaccines are constrained in their ability to provide multiple immunodominant proteins to address emerging pandemic variants or to easily combine multiple pathogens into one vaccine.

To address some of the current limitations of vaccine technologies, we have developed a vaccine platform based on a CRISPR genetically engineered human stem cell, termed the universal vaccine cell (UVC). The principal feature of this vaccine platform is to attempt to reproduce physiologic immunity that is engendered naturally through lytic viral infection and the resulting apoptosis of primary human cells. The platform is designed to deliver an antigenic payload within the context of a physiological apoptotic environment to both release antigen and simultaneously stimulate the host immune response. Here, we use the severe acute respiratory syndrome coronavirus 2 (SARS-CoV-2) virus as a rigorous test platform to demonstrate that this self-adjuvanting, polyvalent UVC can generate a robust and antigen-specific humoral immune response in vaccinated macaques. This vaccine resulted in reduced viral loads in animals challenged with heterologous SARS-CoV-2 Delta variant, which is consistent with current clinical experience with vaccines encoding the WA1/2020 spike against SARS-CoV-2 variants.[29–31]

RESULTS

Genetic engineering of iPSCs to create a cellular vaccine to deliver the SARS-CoV-2 spike antigen

To create a cellular vaccine platform to deliver viral antigens and simultaneously engage host innate immune cells to present these antigens to lymphocytes, we attempted to create a cell with a robust immunogenic phenotype. We selected human induced pluripotent stem cells (iPSCs) as the UVC cell line due to their stable genetics, non-transformed phenotype, ease of genetic engineering, and capacity for rapid, scalable propagation.[32,33] iPSCs also retained the unique ability for programmable differentiation into any cell lineage, thus retaining the future opportunity to explore differentiation of the UVC into different cell types that may have enhanced immunogenic properties.[34]

We first genetically engineered iPSCs to create an immunogenic phenotype by stable integration of the SARS-CoV-2 full-length spike antigen into the AAVS1 safe-harbor locus using CRISPR-Cas9 gene editing (Figure 1A). We selected the original and well-characterized WA1/2020 variant of the SARS-CoV-2 spike antigen sequence with a mutation of the furin cleavage site and proline-stabilizing mutations that are identical to those in the current emergency-use-authorized vaccines being deployed globally to vaccinate against COVID-19[35–37] (Figure S1). By including the spike transmembrane domain sequence in the gene encoding this antigen, we were able to detect high levels of the viral spike on the cell surface of the engineered iPSCs (Figure 1B). This high level of surface viral spike expression was maintained throughout the expansion of the cells and cryopreservation several weeks after CRISPR engineering (data not shown). Spike protein was also readily observed in engineered cell lysates when measured by western blotting (Figure 1C). The yield of antigen released upon lysis was quantified using a spike-specific ELISA assay, and we observed an abundant and dose-dependent release of protein from the cells, which would equate to approximately $\sim$20 μg spike antigen protein delivered in a 10^8 UVC dose (Figure 1D).

To ensure robust delivery of this immunodominant antigen to the recipient immune system, we incorporate an apoptosis-inducing lethal irradiation step during vaccine manufacture by exposing the UVCs to a 10 Gy dose of gamma radiation prior to cryopreservation and vaccination. Thus, when subjects are immunized with the UVC, we reasoned that the cells would undergo apoptosis and release the SARS-CoV-2 spike antigen into the immune microenvironment via production of apoptotic bodies (Figure 1A). In theory, these apoptotic bodies would be phagocytosed by innate immune cells and antigen-presenting cells and be presented to T and B lymphocytes to generate a spike-antigen-specific immune response.

In addition to creating a mechanism for delivery of immunogenic antigens via apoptotic bodies, the irradiation of the UVC is also a safety feature, as it renders the cells unable to proliferate or persist *in vivo* upon vaccination. In support of this, we observed a robust elevation in the proportion of apoptotic cells after 24 and 72 h of culture of irradiated UVC using both apoptotic dyes and flow cytometry (Figure 1E) and by

Figure 1. CRISPR genetic engineering of an iPSC line to create an immunogenic, self-adjuvanting cellular vaccine

(A) Universal vaccine cell CRISPR genetic engineering strategy to create an apoptotic cellular vehicle for antigen delivery.

(B and C) Representative flow cytometric analysis showing expression of SARS-CoV-2 WA1/2020 spike protein on the cell surface (B) and by western blot showing spike protein within UVC whole-cell lysates (C).

(D) ELISA quantification of spike protein released upon UVC lysis for 2 independent UVC cultures.

(E) Proportion of apoptotic cells at 24 and 72 h post-irradiation as measured by 7-AAD staining and flow cytometry.

(F) Morphology, observed by light microscopy, of engineered UVC during expansion culture and, when reseeded into culture 24 h after irradiation, showing apoptosis and cell death.

(G) Absence of detectable proliferation of irradiated UVC as determined by CellTrace yellow proliferation dye staining and measuring the dilution of the dye by flow cytometry over 72 h.

(H) Representative flow cytometric analysis showing deletion of MHC class I and overexpression of MICA on the UVC surface by CRISPR engineering.

(I) Cell counts of 3 independent cultures showing exponential expansion of live engineered UVCs over 21 days in culture.

(J) Relative expression of pluripotency and self-renewal genes by UVC and the control iPSCs from which they were derived, as measured by quantitative PCR, showing maintenance of an iPSC gene expression profile after genetic engineering and expansion. Error bars represent mean ± SEM of 3 technical replicas. All experiments were repeated at least three times.

observation of cell morphology under the microscope (Figure 1F). Furthermore, unlike non-irradiated UVCs, irradiation prevented any detectable proliferation of the cells over 72 h in culture as measured by proliferation dyes using flow cytometry (Figure 1G) and by colony-formation assays (Figure S2). To confirm the absence of proliferation post-irradiation *in vivo*, we transplanted irradiated and non-irradiated UVCs into immunocompetent mice, monitored for teratoma formation over 6 weeks, and showed that neither irradiated nor non-irradiated cells formed tumors in any of the mice evaluated (Figure S3).

Incorporation of NK cell activation signals by genetic engineering to create a self-adjuvanting vaccine cell

In addition to the proposed immunogenicity expected from apoptosis and release of immunogenic antigens upon vaccination, we attempted to increase the immunogenic potential by incorporating a self-adjuvanting phenotype into the UVC. As a form of physiological cell death, apoptosis is generally non-inflammatory.[38] Therefore, to promote effective local inflammation and engage the innate immune system that can mobilize effector cells, we engineered the UVC to mimic a virally infected cell to be recognized and rapidly lysed by host innate immune cells, principally natural killer (NK) cells.[39,40] Many viruses attempt to evade immune recognition by limiting major histocompatibility complex (MHC) class I cell surface expression to reduce the presentation of viral antigens to CD8^{+} T cells.[41,42] This "missing-self" signal can aid in the activation of NK cells and promote cytolysis, and therefore the iPSCs were engineered to completely remove MHC class I molecules from the cell surface via CRISPR knockout of the β2 microglobulin (B2M) gene, a critical component of MHC class I molecules (Figure 1H).

In vivo, lack of MHC class I on the target cell is not sufficient to trigger full NK cell activation alone and a further hallmark of cells undergoing stress or viral infection, is the expression of NK cell activating natural killer group 2 member D (NKG2D) ligands on their cell surface.[43,44] Therefore, the UVC was further engineered to integrate a gene expression cassette in a safe-harbor locus to drive constitutive expression of the human MICA gene (MHC class I polypeptide-related sequence A), a potent activator of NK cells. Using flow cytometry, abundant levels of MICA could be detected on the surface of the engineered UVC (Figure 1H).

Rapid growth kinetics of engineered UVC

Prior to irradiation and cryopreservation of the UVC ready for immunization, we evaluated the growth kinetics of the cells to confirm the capacity for rapid, scalable proliferation that would be needed for a vaccine technology to address the needs of a pandemic. iPSCs are known to have relatively short doubling times in the range of 18–20 h,[45,46] and we observed similar kinetics with an average exponential growth of >50-fold over a 7 day culture period (Figure 1I). Thus, from a starting UVC number of 10^6 cells, the vaccine can be theoretically expanded to provide millions of doses in under 8 weeks and even more quickly if adapted to bioreactor manufacturing.

The consistent rapid cell growth of the UVC and the morphological similarity to unmodified iPSCs suggested the UVC exhibited characteristics of the iPSCs from which they are derived. We thus assessed the stem cell characteristics of the UVC after genetic engineering and rapid expansion to confirm that the cells have retained their original stemness gene expression signatures without acquiring any detectable or obvious changes in phenotype beyond those introduced by genetic engineering. The expanded UVC expressing the SARS-CoV-2 spike antigen, human MICA ligand, and CRISPR knockout of B2M showed a similar level of expression of three important pluripotent transcription factors, NANOG, OCT4, and SOX2, suggesting that they have retained a stem-cell-like transcriptional profile (Figure 1J). Engineered UVCs also showed similar expression to control iPSCs for genes (DCN, vimentin, HES5, and GATA6) that are known to increase in expression as iPSCs differentiate into mesoderm, endoderm, and ectoderm lineages, confirming that the UVCs have a consistent undifferentiated iPSC gene expression profile, morphology, and growth characteristics.[47,48]

Human and primate NK cell cytolysis of UVCs

To further explore the impact of MHC class I loss and overexpression of NK cell ligands on recognition and killing of the UVCs by NK cells, we performed a series of *in vitro* NK cell activation and cytolysis assays. When MHC class I was removed via B2M knockout alone, the UVCs were robustly killed by human NK cells, which increased in an E:T (effector:target) ratio-dependent manner (Figure 2A). We compared the level of UVC cytolysis with that observed with the MHC-deficient K562 leukemia cell line, known to be potent targets for NK cell killing, and found a similar level of cytolysis confirming that the MHC class I-deficient UVCs are readily targeted by NK cells. We extended this analysis to macaque NK cells and found that while control iPSCs (expressing MHC class I) show low levels of killing, the MHC class I knockout UVCs were lysed more readily by the NK cells (Figure 2B).

To assess the relative contribution of overexpressing NK activating ligands on UVC cytolysis by macaque NK cells, we performed an analysis of UVCs transiently overexpressing different NKG2D ligands, including MICA, MICB, and UL16 binding protein 1 (ULBP1). While the level of macrophage inflammatory protein-1β (MIP-1β) was significantly elevated when MICA was overexpressed, proinflammatory and activation markers for NK cells were generally the same regardless of ligand overexpression (Figure 2C). With stable overexpression of MICA by CRISPR engineering, we confirmed a significant increase in total responding macaque NK cells and a significant elevation in MIP-1β (Figure 2D).

Immunogenicity of UVCs in macaques

To evaluate the immunogenicity of the UVCs, we immunized cynomolgus macaques and followed neutralizing and spike-specific antibodies for 6 months. We immunized 9 macaques, aged 6–12 years old, with either 10^7 (n = 3) or 10^8 UVCs (n = 3) expressing the WA1/2020 SARS-COV-2 spike and sham controls (n = 3). Macaques were primed by the intramuscular route without adjuvant at week 0 and were boosted at week 6 (Figure 3A). Neutralizing antibody responses were assessed using a pseudovirus neutralization assay.[49–52] We observed neutralizing antibodies in all UVC vaccinated macaques at week 2 and higher levels at week 4 (Figure 3B). The higher dose of 10^8 UVCs resulted in the most robust titers of neutralizing antibodies at all time points
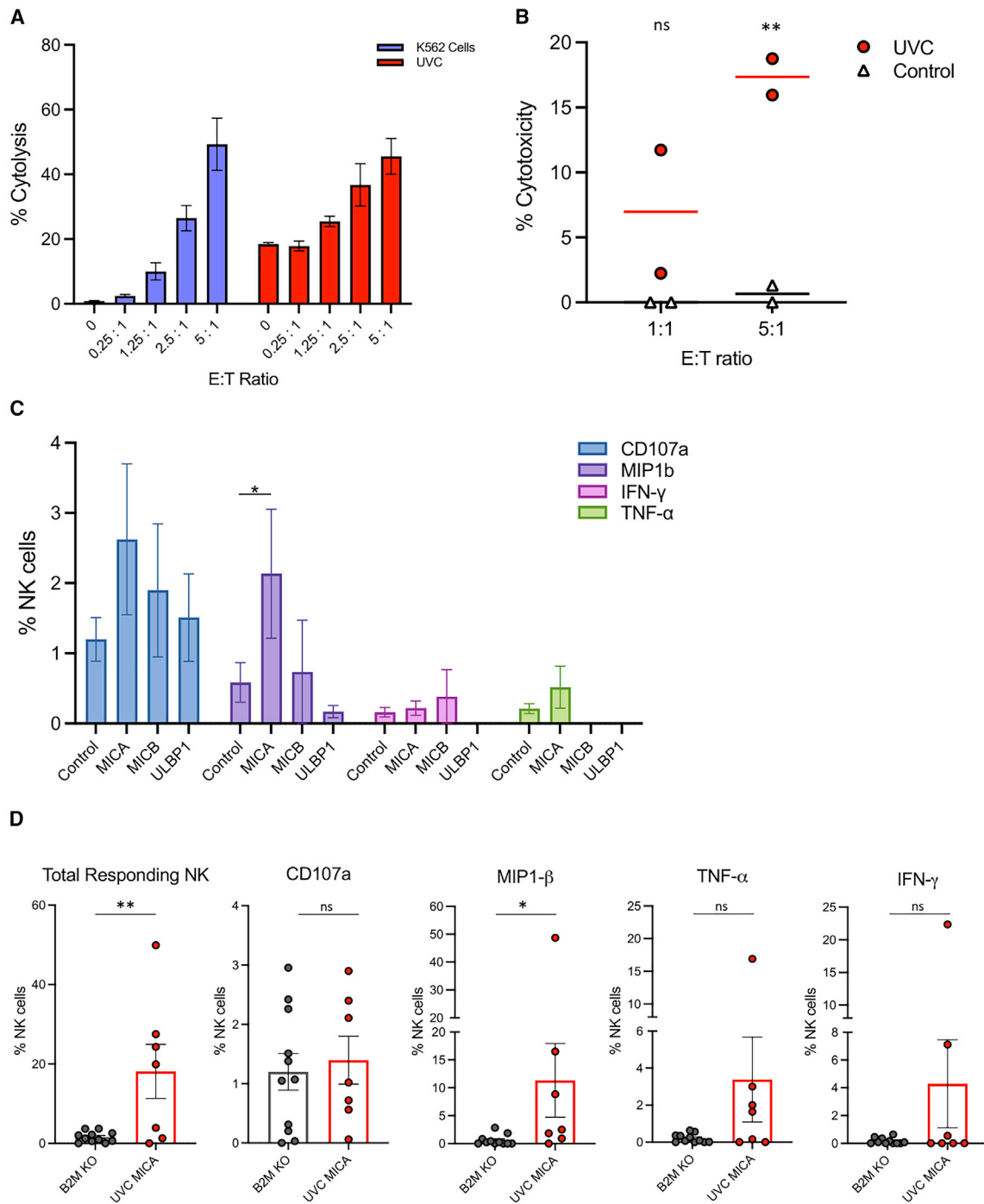
Figure 2. Self-adjuvancy: Enhanced cytolysis of genetically engineered UVC iPSCs via engineered MHC class I deletion and NK apoptotic ligand expression

(A) CRISPR knockout of B2M and loss of MHC class I enhances the killing of UVC cells by human primary NK cells, showing equivalent levels of cytolysis seen with the MHC class I-deficient K562 cell line in 3 independent assays.

(B) A similar elevated cytolysis of MHC-deficient UVC cells is observed with macaque NK cells.

(C) When overexpressed transiently on the UVC, NKG2D family ligands show no elevation in markers of NK cell activation by macaque NK cells, except MICA, which significantly elevates levels of macrophage inflammatory protein-1β (MIP-1β).

(D) When stably overexpressed on the UVC by CRISPR editing, MICA enhanced the NK cell functional responses as measured by ICS of NK cells from 7 macaques. *p < 0.05, **p < 0.01, error bars represent mean ± SEM of 3 biological replicates.
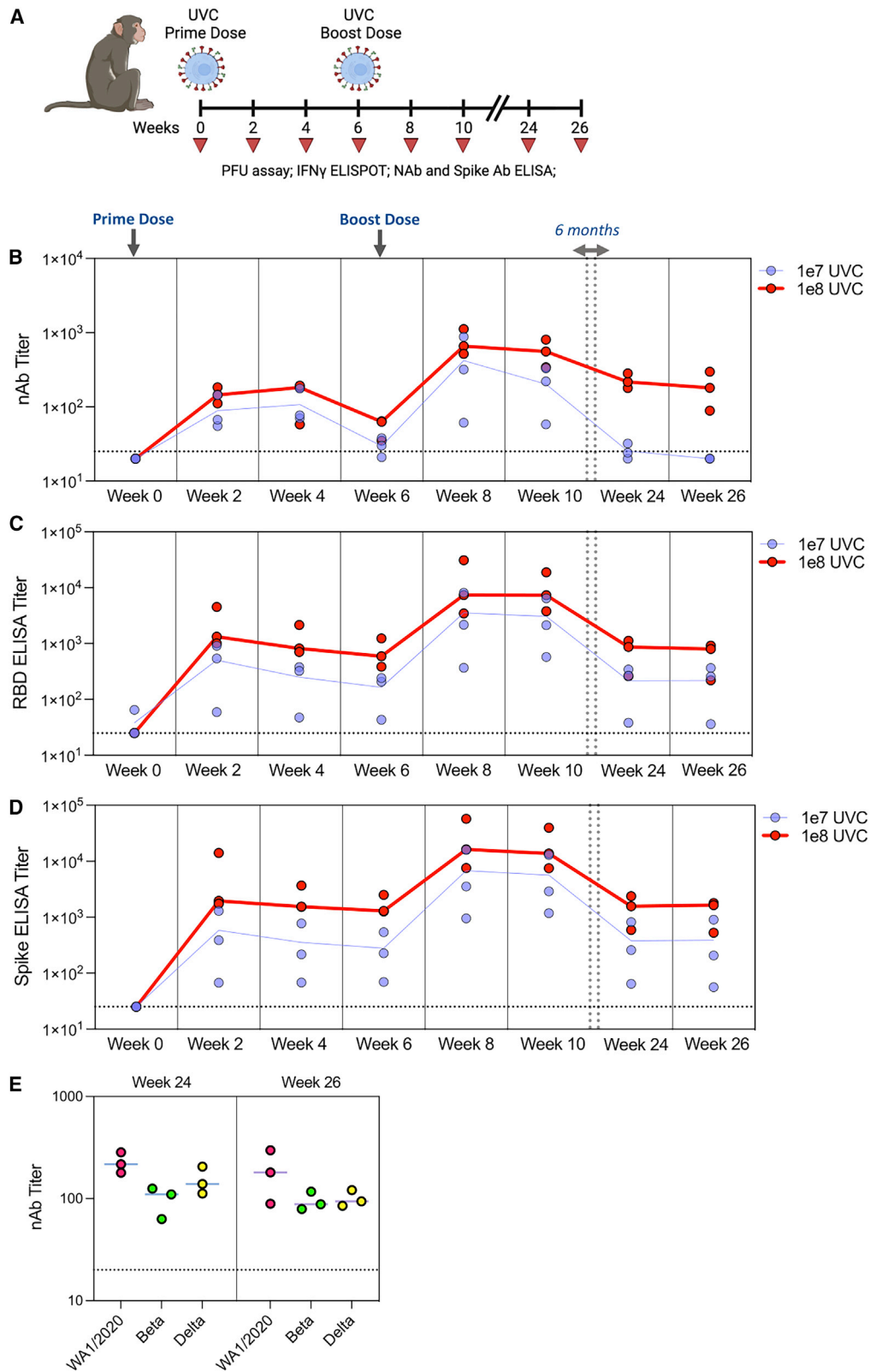
(legend on next page)

tested. Following the boost immunization at week 6, neutralizing antibody titers increased further, reaching titers close to 1,000 with the 10^8 cell dose. Six months after the initial UVC immunization, neutralizing antibodies showed a durable response, particularly for macaques immunized with the 10^8 UVC dose. We also observed robust spike-specific and receptor-binding domain (RBD)-specific antibody titers as measured by enzyme-linked immunosorbent assay (ELISA) in vaccinated animals (Figures 3C and 3D). At 6 months after immunization, detectable levels of neutralizing antibodies against Beta and Delta variants were also observed, albeit lower than seen with the immunizing antigen variant WA1/2020 spike, suggesting that humoral immunity is also generated against SARS-CoV-2 variants (Figure 3E).

Protective efficacy against heterologous SARS-CoV-2 challenge

In a second macaque study, we immunized 12 rhesus macaques, aged 6–12 years old, with 10^8 UVCs (n = 6) expressing the SARS-CoV-2 WA1/2020 spike antigen and sham controls (n = 6) (Figure 4A). At week 8, the macaques were challenged with 10^5 50% tissue culture infectious dose ($TCID_{50}$) of heterologous SARS-CoV-2 B.1.617.2 (Delta) by intranasal and intratracheal routes.[51,52] In addition to measuring neutralizing antibodies (Figure S4), viral loads in bronchoalveolar lavage (BAL) and nasal swabs were assessed by reverse transcription PCR (RT-PCR) specific for subgenomic mRNA (sgRNA), which is thought to measure replicating virus.[52,53] Sham controls showed a median peak of 5.39 (range 4.60–5.88) $\log_{10}$ sgRNA copies/mL in BAL samples (Figures 4B and 4D). In macaques immunized with the UVC, a significantly lower level of virus was detected in BAL samples, with a median peak of 2.78 (range 1.70–4.63) $\log_{10}$ sgRNA copies/mL, representing a 2.81 log reduction in virus in UVC-vaccinated animals (p = 0.0152). A significant 0.96 log reduction of virus was also observed in nasal swabs from UVC-immunized macaques compared with sham controls (Figures 4C and 4E; p = 0.0260). These data demonstrate that a two-dose regimen of UVC promoted antigen-specific antibody responses with levels of neutralizing antibodies and durability similar to current approved COVID-19 vaccines, and this can lead to partial protection against a heterologous SARS-CoV-2 Delta challenge.[49,54,55]

DISCUSSION

The global need for improved vaccine technologies to meet future pandemics is driving a renaissance of innovation in vaccinology. COVID-19 has demonstrated the rapid pace at which viral mutations can accumulate and new variants emerge that can escape the protective efficacy of existing vaccines designed against earlier viral antigen sequences.[10,11,29–31,56,57] To address the need for novel vaccine technologies, we developed a UVC platform technology to generate immunity via self-adjuvancy through apoptosis and NK-cell-mediated cytolysis within the immune microenvironment.

Our data demonstrate that the UVC vaccine platform can induce robust neutralizing antibody responses in macaques when delivering the SARS-CoV-2 WA1/2020[58] spike that contains a mutation of the furin cleavage site and two proline-stabilizing mutations.[35–37] The neutralizing antibody titers around 1,000 are similar to those reported for the current COVID-19 mRNA vaccines.[49,54,55] Following a high dose, heterologous SARS-CoV-2 Delta challenge, the UVC vaccine reduced viral loads 2.81 logs in the BAL and 0.96 logs in nasal swabs. The more robust protection in the lower respiratory tract compared with the upper respiratory tract is consistent with clinical data showing that all current COVID-19 vaccines are better at protecting against severe disease than infection with emerging SARS-CoV-2 variants.[29,31] A prior study showed that the Moderna mRNA-1273 vaccine resulted in an approximate 3 log reduction in viral loads in BAL and a 1 log reduction in nasal swabs against a heterologous SARS-CoV-2 Delta challenge in macaques, which appears similar to our data with UVC.

Regarding safety, the UVC undergoes lethal irradiation during manufacture and rapid apoptosis in the immune microenvironment upon vaccination. This is the principal mechanism of efficacy of the UVC and provides an important safety feature with no detectable persistence or teratogenicity. The irradiation-induced apoptosis is further enhanced by CRISPR genetic engineering to remove MHC class I expression and introduce cell surface expression of the NKG2D ligand MICA, making the UVCs potent targets for host NK cells. Recruited NK cells will likely recognize the UVCs as virally infected cells through MHC class I absence and MICA activation of NKG2D signaling to mediate a direct killing effect and release of protein antigen.[59] The apoptosis- and NK-mediated cytolysis enables the UVC to be a self-adjuvanting vaccine vector without the need for additional chemicals adjuvants or additional foreign antigens. Thus, the UVC may mimic the physiological engagement of the immune system typical of virally infected cells within the tissues of an individual suffering with the disease.

The CRISPR genetic engineering to render the UVC highly immunogenic and self-adjuvanting also presents a unique opportunity to address antigen polyvalency. Unlike mRNA or DNA vaccines or recombinant viral vector vaccines, which have limits on the size or number of independent encoded antigens they can deliver, the UVC can be engineered to deliver a higher number of full-length protein antigens. Thus, there is the ability to create polyvalency against multiple epitopes in a rapid modular gene

---

Figure 3. Humoral immune responses in UVC-vaccinated macaques

(A) Macaques received a high WA1/2020 spike expressing UVC prime dose (10^8) or low UVC prime dose (10^7) at week 0 and a boost dose matched to that of the prime dose at week 6.

(B–D) Humoral immune responses were assessed at 2 week intervals up to week 10 and then again at weeks 24 and 26 by (B) pseudovirus neutralization assays and (C) RBD-specific and (D) spike-binding antibody ELISA.

(E) In addition to the WA1/2020 SARS-CoV-2 variant, detectable neutralizing antibodies against the B.1.351 (Beta) and B.1.617.2 (Delta) variants were observed in immunized macaques at weeks 24 and 26. Red bars reflect median responses. Dotted lines reflect assay limit of quantification. Data points represent individual primates, 3 per group. NAb, neutralizing antibody.
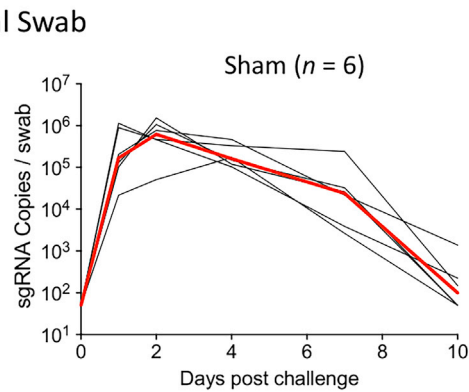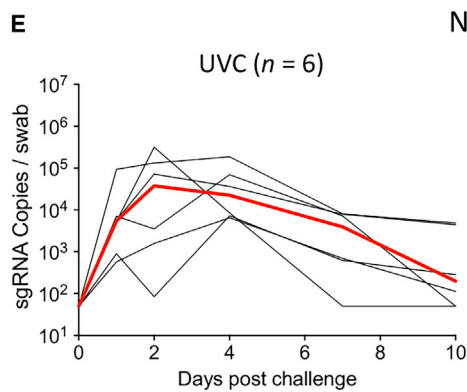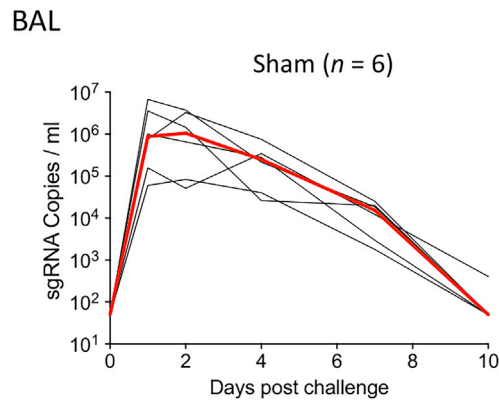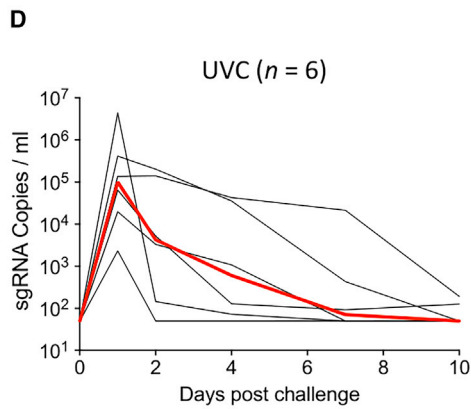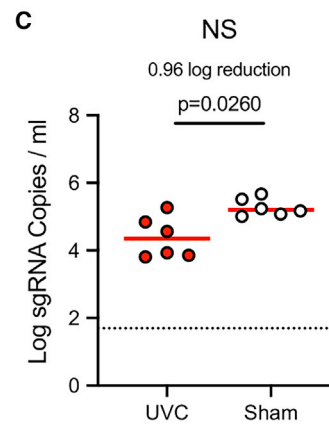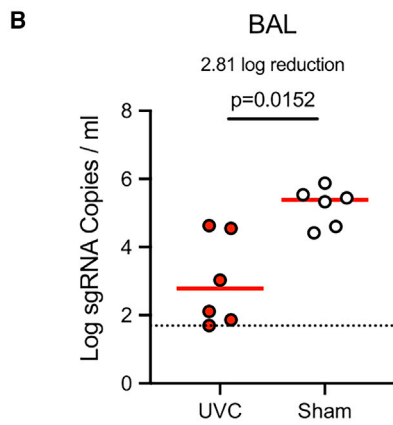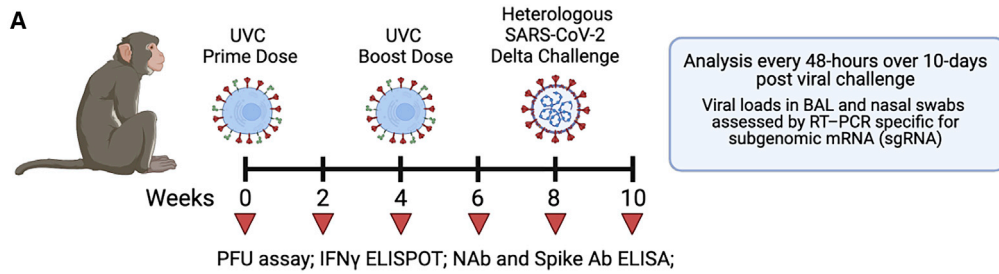
(legend on next page)

cassette fashion through CRISPR engineering of the iPSC genome.

A perceived limitation of the UVC technology may be the seemingly complex and costly nature of developing and manufacturing a human cell as a vector for vaccination at scale. However, the UVC is a cell line, not a complex cell therapy, and can thus be scaled within appropriate parameters for such a biologic agent. The UVC cell line can be expanded rapidly to scale with predictable growth kinetics and quality assurance/quality control (QA/QC) controls. The modular nature of the UVC and the ability to integrate emerging viral antigens into the cellular genome using CRISPR can allow scalable manufacture of new polyvalent vaccines to address emerging variants. In fact, the genetic engineering of the UVCs can be accomplished in a matter of weeks prior to exponential cell culture expansion to create millions of clinical doses. Moreover, quantification of viral spike protein released from lysed UVCs suggests that a 10^8 UVC number can deliver an antigen dose comparable to, and in excess of, that administered by other approved COVID-19 protein vaccines. At the 10^8 UVC dose, billions of doses could theoretically be generated under good manufacturing practice (GMP) conditions in under 8 weeks.

In summary, our data establish a cellular vaccine platform and demonstrate that immunization with UVC expressing the WA1/2020 SARS-CoV-2 spike elicits robust neutralizing antibody responses that provide partial protection against heterologous Delta SARS-CoV-2 challenge in rhesus macaques. This platform offers a unique class of gene and cell therapy prophylaxis for potential future viral pandemics.

Limitations of the study

One limitation of this study is that we have yet to observe the generation of a robust T cell response in animals vaccinated with the UVC. The measurable, albeit modest, CD8^{+} T cell responses seen with the adenoviral and mRNA vaccines for COVID-19 have not resulted in neutralizing antibody (nAb) titers and duration of protection longer than 6–9 months.[8,60] One potential hypothesis to begin to establish a clinically meaningful cellular response is to explore in future studies non-spike antigens, leveraging the simultaneous polyvalency of the UVC platform, including immunodominant T cell epitopes such as those in the nucleocapsid and viral accessory proteins.[61–63]

Another limitation of this study is that investigation into persistence of irradiated UVCs in animal models was limited to immunocompetent mice, selected because they represent the target population of this vaccine technology: healthy individuals with an intact immune system. Immunocompromised animals lacking cells of the adaptive immune system may not clear injected cells as effectively, and although lethal irradiation of the UVC designed to induce apoptosis and prevent cell survival is likely to

prevent any persistence and proliferation of cells in recipients, this has yet to be addressed experimentally.

STAR★METHODS

Detailed methods are provided in the online version of this paper and include the following:

- **KEY RESOURCES TABLE**
- **RESOURCE AVAILABILITY**
  - Lead contact
  - Materials availability
  - Data and code availability
- **EXPERIMENTAL MODEL AND SUBJECT DETAILS**
  - Cell lines
  - Animals and study design
- **METHOD DETAILS**
  - iPS cell irradiation and cryopreservation
  - CRISPR genetic engineering
  - Intracellular spike protein staining
  - Flow cytometry analysis of cell surface antigen expression
  - Western blot
  - qPCR measurement of stem cell factors
  - SARS-CoV-2 spike protein ELISA
  - UVC proliferation and apoptosis assays
  - Colony formation assay
  - CAM cytotoxicity assay
  - Nucleofection of NKG2D ligands in iPS cells
  - NK cell intracellular cytokine staining assay
  - Immunohistochemical analysis
  - Subgenomic viral mRNA assay
  - Serum antibody ELISA
  - Pseudovirus neutralization assay
- **QUANTIFICATION AND STATISTICAL ANALYSIS**

AUTHOR CONTRIBUTIONS

Genetic engineering and *in vitro* characterization of the UVC were led by T.H., with A.C., A.S., E.L., K.C., R.G., and E.A. generating and interpreting experimental data and performing statistical analysis. R.K.R. designed and led the NK cell killing assays, with C.M., K.K., and M.M. generating and interpreting experimental data. The vaccination study was designed and led by D.H.B.

Figure 4. Viral loads in UVC-vaccinated macaques after heterologous SARS-CoV-2 challenge
(A) Rhesus macaques were immunized with 10^8 WA1/2020 spike expressing UVCs at week 0 and received a boost dose of 10^8 matched UVCs at week 4. Macaques were then challenged at week 6 by intranasal and intratracheal routes with 1.0×10^5 TCID$_{50}$ of SARS-CoV-2 B.1.617.2 (Delta).
(B and C) Log$_{10}$(sgRNA [copies per mL]) (limit of quantification 50 copies per mL) were assessed, and peak viral loads are shown in (B) bronchoalveolar lavage (BAL) samples and (C) nasal swabs (NSs) in sham controls and vaccinated macaques after challenge.
(D and E) Viral loads were assessed every 2 days. Dotted lines reflect assay limit of quantification. Data points represent individual primates, 6 per group. NAb, neutralizing antibody.

Immunologic and virologic assays were led by A.C., J.Y., K.M., and V.G. Humoral immune responses were assessed by K.M. and J.Y. The paper was written by T.H., D.H.B., and M.C., with the involvement of all co-authors.

REFERENCES

1. Polack, F.P., Thomas, S.J., Kitchin, N., Absalon, J., Gurtman, A., Lockhart, S., Perez, J.L., Pérez Marc, G., Moreira, E.D., Zerbini, C., et al. (2020). Safety and efficacy of the BNT162b2 mRNA covid-19 vaccine. N. Engl. J. Med. 383, 2603–2615. https://doi.org/10.1056/NEJMoa2034577.

2. Baden, L.R., El Sahly, H.M., Essink, B., Kotloff, K., Frey, S., Novak, R., Diemert, D., Spector, S.A., Rouphael, N., Creech, C.B., et al. (2021). Efficacy and safety of the mRNA-1273 SARS-CoV-2 vaccine. N. Engl. J. Med. 384, 403–416. https://doi.org/10.1056/NEJMoa2035389.

3. Sadoff, J., Gray, G., Vandebosch, A., Cárdenas, V., Shukarev, G., Grinsztejn, B., Goepfert, P.A., Truyers, C., Fennema, H., Spiessens, B., et al. (2021). Safety and efficacy of single-dose Ad26.COV2.S vaccine against covid-19. N. Engl. J. Med. 384, 2187–2201. https://doi.org/10.1056/NEJMoa2101544.

4. Levin, E.G., Lustig, Y., Cohen, C., Fluss, R., Indenbaum, V., Amit, S., Doolman, R., Asraf, K., Mendelson, E., Ziv, A., et al. (2021). Waning immune humoral response to BNT162b2 covid-19 vaccine over 6 months. N. Engl. J. Med. 385, e84. https://doi.org/10.1056/NEJMoa2114583.

5. Naaber, P., Tserel, L., Kangro, K., Sepp, E., Jürjenson, V., Adamson, A., Haljasmägi, L., Rumm, A.P., Maruste, R., Kärner, J., et al. (2021). Dynamics of antibody response to BNT162b2 vaccine after six months: a longitudinal prospective study. Lancet Reg. Health. Eur. 10, 100208. https://doi.org/10.1016/j.lanepe.2021.100208.

6. Thomas, S.J., Moreira, E.D., Jr., Kitchin, N., Absalon, J., Gurtman, A., Lockhart, S., Perez, J.L., Pérez Marc, G., Polack, F.P., Zerbini, C., et al. (2021). Safety and efficacy of the BNT162b2 mRNA covid-19 vaccine through 6 months. N. Engl. J. Med. 385, 1761–1773. https://doi.org/10.1056/NEJMoa2110345.

7. Cohn, B.A., Cirillo, P.M., Murphy, C.C., Krigbaum, N.Y., and Wallace, A.W. (2022). SARS-CoV-2 vaccine protection and deaths among US veterans during 2021. Science 375, 331–336. https://doi.org/10.1126/science.abm0620.

8. Collier, A.R.Y., Yu, J., McMahan, K., Liu, J., Chandrashekar, A., Maron, J.S., Atyeo, C., Martinez, D.R., Ansel, J.L., Aguayo, R., et al. (2021). Differential kinetics of immune responses elicited by covid-19 vaccines. N. Engl. J. Med. 385, 2010–2012. https://doi.org/10.1056/NEJMc2115596.

9. Barouch, D.H., Stephenson, K.E., Sadoff, J., Yu, J., Chang, A., Gebre, M., McMahan, K., Liu, J., Chandrashekar, A., Patel, S., et al. (2021). Durable humoral and cellular immune responses 8 Months after Ad26.COV2.S vaccination. N. Engl. J. Med. 385, 951–953. https://doi.org/10.1056/NEJMc2108829.

10. Planas, D., Veyer, D., Baidaliuk, A., Staropoli, I., Guivel-Benhassine, F., Rajah, M.M., Planchais, C., Porrot, F., Robillard, N., Puech, J., et al. (2021). Reduced sensitivity of SARS-CoV-2 variant Delta to antibody neutralization. Nature 596, 276–280. https://doi.org/10.1038/s41586-021-03777-9.

11. Callaway, E. (2021). Heavily mutated Omicron variant puts scientists on alert. Nature 600, 21. https://doi.org/10.1038/d41586-021-03552-w.

12. Lefèvre, B., Tondeur, L., Madec, Y., Grant, R., Lina, B., van der Werf, S., Rabaud, C., and Fontanet, A. (2021). Beta SARS-CoV-2 variant and BNT162b2 vaccine effectiveness in long-term care facilities in France. Lancet. Healthy Longev. 2, e685–e687. https://doi.org/10.1016/S2666-7568(21)00230-0.

13. Abu-Raddad, L.J., Chemaitelly, H., and Butt, A.A.; National Study Group for COVID-19 Vaccination (2021). Effectiveness of the BNT162b2 covid-19 vaccine against the B.1.1.7 and B.1.351 variants. N. Engl. J. Med. 385, 187–189. https://doi.org/10.1056/NEJMc2104974.

14. Villarreal, R., and Casale, T.B. (2020). Commonly used adjuvant human vaccines: advantages and side effects. J. Allergy Clin. Immunol. Pract. 8, 2953–2957. https://doi.org/10.1016/j.jaip.2020.04.045.

15. Lauer, K.B., Borrow, R., and Blanchard, T.J. (2017). Multivalent and multipathogen viral vector vaccines. Clin. Vaccine Immunol. 24, e00298-16. https://doi.org/10.1128/CVI.00298-16.

16. Schlingmann, B., Castiglia, K.R., Stobart, C.C., and Moore, M.L. (2018). Polyvalent vaccines: high-maintenance heroes. PLoS Pathog. 14, e1006904. https://doi.org/10.1371/journal.ppat.1006904.

17. Pardi, N., Hogan, M.J., Porter, F.W., and Weissman, D. (2018). mRNA vaccines - a new era in vaccinology. Nat. Rev. Drug Discov. 17, 261–279. https://doi.org/10.1038/nrd.2017.243.

18. Pulendran, B., S Arunachalam, P., and O'Hagan, D.T. (2021). Emerging concepts in the science of vaccine adjuvants. Nat. Rev. Drug Discov. 20, 454–475. https://doi.org/10.1038/s41573-021-00163-y.

19. Yousefi Avarvand, A., Meshkat, Z., Khademi, F., and Tafaghodi, M. (2021). Immunogenicity of HspX/EsxS fusion protein of Mycobacterium tuberculosis along with ISCOMATRIX and PLUSCOM nano-adjuvants after subcutaneous administration in animal model. Microb. Pathog. 154, 104842. https://doi.org/10.1016/j.micpath.2021.104842.

20. Cebon, J.S., Gore, M., Thompson, J.F., Davis, I.D., McArthur, G.A., Walpole, E., Smithers, M., Cerundolo, V., Dunbar, P.R., MacGregor, D., et al. (2020). Results of a randomized, double-blind phase II clinical trial of NY-ESO-1 vaccine with ISCOMATRIX adjuvant versus ISCOMATRIX alone in participants with high-risk resected melanoma. J. Immunother. Cancer 8, e000410. https://doi.org/10.1136/jitc-2019-000410.

21. Baz Morelli, A., Becher, D., Koernig, S., Silva, A., Drane, D., and Maraskovsky, E. (2012). ISCOMATRIX: a novel adjuvant for use in prophylactic and therapeutic vaccines against infectious diseases. J. Med. Microbiol. 61, 935–943. https://doi.org/10.1099/jmm.0.040857-0.

22. O'Hagan, D.T., Lodaya, R.N., and Lofano, G. (2020). The continued advance of vaccine adjuvants - 'we can work it out. Semin. Immunol. 50, 101426. https://doi.org/10.1016/j.smim.2020.101426.

23. Zhou, F., Hansen, L., Pedersen, G., Grødeland, G., and Cox, R. (2021). Matrix M adjuvanted H5N1 vaccine elicits broadly neutralizing antibodies and neuraminidase inhibiting antibodies in humans that correlate with in vivo protection. Front. Immunol. 12, 747774. https://doi.org/10.3389/fimmu.2021.747774.

24. Bengtsson, K.L., Song, H., Stertman, L., Liu, Y., Flyer, D.C., Massare, M.J., Xu, R.H., Zhou, B., Lu, H., Kwilas, S.A., et al. (2016). Matrix-M adjuvant enhances antibody, cellular and protective immune responses of a Zaire Ebola/Makona virus glycoprotein (GP) nanoparticle vaccine in mice. Vaccine 34, 1927–1935. https://doi.org/10.1016/j.vaccine.2016.02.033.

25. Pavord, S., Scully, M., Hunt, B.J., Lester, W., Bagot, C., Craven, B., Rampotas, A., Ambler, G., and Makris, M. (2021). Clinical features of vaccine-induced immune thrombocytopenia and thrombosis. N. Engl. J. Med. 385, 1680–1689. https://doi.org/10.1056/NEJMoa2109908.

26. Long, B., Bridwell, R., and Gottlieb, M. (2021). Thrombosis with thrombocytopenia syndrome associated with COVID-19 vaccines. Am. J. Emerg. Med. 49, 58–61. https://doi.org/10.1016/j.ajem.2021.05.054.

27. Cattaneo, M. (2021). Thrombosis with Thrombocytopenia Syndrome associated with viral vector COVID-19 vaccines. Eur. J. Intern. Med. 89, 22–24. https://doi.org/10.1016/j.ejim.2021.05.031.

28. Afkhami, S., Yao, Y., and Xing, Z. (2016). Methods and clinical development of adenovirus-vectored vaccines against mucosal pathogens. Mol. Ther. Methods Clin. Dev. *3*, 16030. https://doi.org/10.1038/mtm.2016.30.

29. Lopez Bernal, J., Gower, C., and Andrews, N.; Public Health England Delta Variant Vaccine Effectiveness Study Group (2021). Effectiveness of covid-19 vaccines against the B.1.617.2 (Delta) variant. N. Engl. J. Med. *385*, e92. https://doi.org/10.1056/NEJMc2113090.

30. Grant, R., Charmet, T., Schaeffer, L., Galmiche, S., Madec, Y., Von Platen, C., Chény, O., Omar, F., David, C., Rogoff, A., et al. (2022). Impact of SARS-CoV-2 Delta variant on incubation, transmission settings and vaccine effectiveness: results from a nationwide case-control study in France. Lancet Reg. Health. Eur. *13*, 100278. https://doi.org/10.1016/j.lanepe.2021.100278.

31. Fowlkes, A., Gaglani, M., Groover, K., Thiese, M.S., Tyner, H., and Ellingson, K.; HEROES-RECOVER Cohorts (2021). Effectiveness of COVID-19 vaccines in preventing SARS-CoV-2 infection among frontline workers before and during B.1.617.2 (Delta) variant predominance - eight U.S. Locations, December 2020-August 2021. MMWR Morb. Mortal. Wkly. Rep. *70*, 1167–1169. https://doi.org/10.15585/mmwr.mm7034e4.

32. Abu-Dawud, R., Graffmann, N., Ferber, S., Wruck, W., and Adjaye, J. (2018). Pluripotent stem cells: induction and self-renewal. Philos. Trans. R. Soc. Lond. B Biol. Sci. *373*, 20170213. https://doi.org/10.1098/rstb.2017.0213.

33. Deinsberger, J., Reisinger, D., and Weber, B. (2020). Global trends in clinical trials involving pluripotent stem cells: a systematic multi-database analysis. NPJ Regen. Med. *5*, 15. https://doi.org/10.1038/s41536-020-00100-4.

34. Shi, Y., Inoue, H., Wu, J.C., and Yamanaka, S. (2017). Induced pluripotent stem cell technology: a decade of progress. Nat. Rev. Drug Discov. *16*, 115–130. https://doi.org/10.1038/nrd.2016.245.

35. Kirchdoerfer, R.N., Cottrell, C.A., Wang, N., Pallesen, J., Yassine, H.M., Turner, H.L., Corbett, K.S., Graham, B.S., McLellan, J.S., and Ward, A.B. (2016). Pre-fusion structure of a human coronavirus spike protein. Nature *531*, 118–121. https://doi.org/10.1038/nature17200.

36. Pallesen, J., Wang, N., Corbett, K.S., Wrapp, D., Kirchdoerfer, R.N., Turner, H.L., Cottrell, C.A., Becker, M.M., Wang, L., Shi, W., et al. (2017). Immunogenicity and structures of a rationally designed prefusion MERS-CoV spike antigen. Proc. Natl. Acad. Sci. USA *114*, E7348–E7357. https://doi.org/10.1073/pnas.1707304114.

37. Wrapp, D., Wang, N., Corbett, K.S., Goldsmith, J.A., Hsieh, C.L., Abiona, O., Graham, B.S., and McLellan, J.S. (2020). Cryo-EM structure of the 2019-nCoV spike in the prefusion conformation. Preprint at bioRxiv. https://doi.org/10.1101/2020.02.11.944462.

38. Szondy, Z., Sarang, Z., Kiss, B., Garabuczi, É., and Köröskényi, K. (2017). Anti-inflammatory mechanisms triggered by apoptotic cells during their clearance. Front. Immunol. *8*, 909. https://doi.org/10.3389/fimmu.2017.00909.

39. Brandstadter, J.D., and Yang, Y. (2011). Natural killer cell responses to viral infection. J. Innate Immun. *3*, 274–279. https://doi.org/10.1159/000324176.

40. Waggoner, S.N., Reighard, S.D., Gyurova, I.E., Cranert, S.A., Mahl, S.E., Karmele, E.P., McNally, J.P., Moran, M.T., Brooks, T.R., Yaqoob, F., and Rydzynski, C.E. (2016). Roles of natural killer cells in antiviral immunity. Curr. Opin. Virol. *16*, 15–23. https://doi.org/10.1016/j.coviro.2015.10.008.

41. Koutsakos, M., McWilliam, H.E.G., Aktepe, T.E., Fritzlar, S., Illing, P.T., Mifsud, N.A., Purcell, A.W., Rockman, S., Reading, P.C., Vivian, J.P., et al. (2019). Downregulation of MHC class I expression by influenza A and B viruses. Front. Immunol. *10*, 1158. https://doi.org/10.3389/fimmu.2019.01158.

42. Schuren, A.B., Costa, A.I., and Wiertz, E.J. (2016). Recent advances in viral evasion of the MHC Class I processing pathway. Curr. Opin. Immunol. *40*, 43–50. https://doi.org/10.1016/j.coi.2016.02.007.

43. Paul, S., and Lal, G. (2017). The molecular mechanism of natural killer cells function and its importance in cancer immunotherapy. Front. Immunol. *8*, 1124. https://doi.org/10.3389/fimmu.2017.01124.

44. Wensveen, F.M., Jelenčić, V., and Polić, B. (2018). NKG2D: a master regulator of immune cell responsiveness. Front. Immunol. *9*, 441. https://doi.org/10.3389/fimmu.2018.00441.

45. Chatterjee, I., Li, F., Kohler, E.E., Rehman, J., Malik, A.B., and Wary, K.K. (2016). Induced pluripotent stem (iPS) cell culture methods and induction of differentiation into endothelial cells. Methods Mol. Biol. *1357*, 311–327. https://doi.org/10.1007/7651_2015_203.

46. Rivera, T., Zhao, Y., Ni, Y., and Wang, J. (2020). Human-induced pluripotent stem cell culture methods under cGMP conditions. Curr. Protoc. Stem Cell Biol. *54*, e117. https://doi.org/10.1002/cpsc.117.

47. Swaidan, N.T., Salloum-Asfar, S., Palangi, F., Errafii, K., Soliman, N.H., Aboughalia, A.T., Wali, A.H.S., Abdulla, S.A., and Emara, M.M. (2020). Identification of potential transcription factors that enhance human iPSC generation. Sci. Rep. *10*, 21950. https://doi.org/10.1038/s41598-020-78932-9.

48. Shi, G., and Jin, Y. (2010). Role of Oct4 in maintaining and regaining stem cell pluripotency. Stem Cell Res. Ther. *1*, 39. https://doi.org/10.1186/scrt39.

49. Mercado, N.B., Zahn, R., Wegmann, F., Loos, C., Chandrashekar, A., Yu, J., Liu, J., Peter, L., McMahan, K., Tostanoski, L.H., et al. (2020). Single-shot Ad26 vaccine protects against SARS-CoV-2 in rhesus macaques. Nature *586*, 583–588. https://doi.org/10.1038/s41586-020-2607-z.

50. Yang, Z.Y., Kong, W.P., Huang, Y., Roberts, A., Murphy, B.R., Subbarao, K., and Nabel, G.J. (2004). A DNA vaccine induces SARS coronavirus neutralization and protective immunity in mice. Nature *428*, 561–564. https://doi.org/10.1038/nature02463.

51. Yu, J., Tostanoski, L.H., Peter, L., Mercado, N.B., McMahan, K., Mahrokhian, S.H., Nkolola, J.P., Liu, J., Li, Z., Chandrashekar, A., et al. (2020). DNA vaccine protection against SARS-CoV-2 in rhesus macaques. Science *369*, 806–811. https://doi.org/10.1126/science.abc6284.

52. Chandrashekar, A., Liu, J., Martinot, A.J., McMahan, K., Mercado, N.B., Peter, L., Tostanoski, L.H., Yu, J., Maliga, Z., Nekorchuk, M., et al. (2020). SARS-CoV-2 infection protects against rechallenge in rhesus macaques. Science *369*, 812–817. https://doi.org/10.1126/science.abc4776.

53. Wölfel, R., Corman, V.M., Guggemos, W., Seilmaier, M., Zange, S., Müller, M.A., Niemeyer, D., Jones, T.C., Vollmar, P., Rothe, C., et al. (2020). Virological assessment of hospitalized patients with COVID-2019. Nature *581*, 465–469. https://doi.org/10.1038/s41586-020-2196-x.

54. Vogel, A.B., Kanevsky, I., Che, Y., Swanson, K.A., Muik, A., Vormehr, M., Kranz, L.M., Walzer, K.C., Hein, S., Güler, A., et al. (2021). BNT162b vaccines protect rhesus macaques from SARS-CoV-2. Nature *592*, 283–289. https://doi.org/10.1038/s41586-021-03275-y.

55. Corbett, K.S., Flynn, B., Foulds, K.E., Francica, J.R., Boyoglu-Barnum, S., Werner, A.P., Flach, B., O'Connell, S., Bock, K.W., Minai, M., et al. (2020). Evaluation of the mRNA-1273 vaccine against SARS-CoV-2 in nonhuman primates. N. Engl. J. Med. *383*, 1544–1555. https://doi.org/10.1056/NEJMoa2024671.

56. Wang, L., and Cheng, G. (2022). Sequence analysis of the emerging sars-CoV-2 variant omicron in South Africa. J. Med. Virol. *94*, 1728–1733. https://doi.org/10.1002/jmv.27516.

57. CDC COVID-19 Response Team (2021). SARS-CoV-2 B.1.1.529 (omicron) variant - United States, December 1-8, 2021. MMWR Morb. Mortal. Wkly. Rep. *70*, 1731–1734. https://doi.org/10.15585/mmwr.mm7050e1.

58. Huang, C., Wang, Y., Li, X., Ren, L., Zhao, J., Hu, Y., Zhang, L., Fan, G., Xu, J., Gu, X., et al. (2020). Clinical features of patients infected with 2019 novel coronavirus in Wuhan, China. Lancet *395*, 497–506. https://doi.org/10.1016/S0140-6736(20)30183-5.

59. Björkström, N.K., Strunz, B., and Ljunggren, H.G. (2022). Natural killer cells in antiviral immunity. Nat. Rev. Immunol. *22*, 112–123. https://doi.org/10.1038/s41577-021-00558-3.

60. Tartof, S.Y., Slezak, J.M., Fischer, H., Hong, V., Ackerson, B.K., Ranasinghe, O.N., Frankland, T.B., Ogun, O.A., Zamparo, J.M., Gray, S., et al. (2021). Effectiveness of mRNA BNT162b2 COVID-19 vaccine up to 6 months in a large integrated health system in the USA: a retrospective cohort study. Lancet *398*, 1407–1416. https://doi.org/10.1016/S0140-6736(21)02183-8.

61. Smits, V.A.J., Hernández-Carralero, E., Paz-Cabrera, M.C., Cabrera, E., Hernández-Reyes, Y., Hernández-Fernaud, J.R., Gillespie, D.A., Salido, E., Hernández-Porto, M., and Freire, R. (2021). The Nucleocapsid protein triggers the main humoral immune response in COVID-19 patients. Biochem. Biophys. Res. Commun. *543*, 45–49. https://doi.org/10.1016/j.bbrc.2021.01.073.

62. Vidal, S.J., Collier, A.R.Y., Yu, J., McMahan, K., Tostanoski, L.H., Ventura, J.D., Aid, M., Peter, L., Jacob-Dolan, C., Anioke, T., et al. (2021). Correlates of neutralization against SARS-CoV-2 variants of concern by early pandemic sera. J. Virol. *95*, e0040421. https://doi.org/10.1128/JVI.00404-21.

63. Lu, S., Xie, X.X., Zhao, L., Wang, B., Zhu, J., Yang, T.R., Yang, G.W., Ji, M., Lv, C.P., Xue, J., et al. (2021). The immunodominant and neutralization linear epitopes for SARS-CoV-2. Cell Rep. *34*, 108666. https://doi.org/10.1016/j.celrep.2020.108666.

64. Chandrashekar, A., Yu, J., McMahan, K., Jacob-Dolan, C., Liu, J., He, X., Hope, D., Anioke, T., Barrett, J., Chung, B., et al. (2022). Vaccine protection against the SARS-CoV-2 Omicron variant in macaques. Cell *185*, 1549–1555.e11. https://doi.org/10.1016/j.cell.2022.03.024.

STAR★METHODS

KEY RESOURCES TABLE

REAGENT or RESOURCE	SOURCE	IDENTIFIER
Antibodies		
Rabbit Anti-SARS-CoV-2 Spike Glycoprotein S1 antibody	Abcam	Cat# ab275759; RRID:AB_2892127
Goat Anti-Rabbit IgG H&L Alexa 488	Abcam	Cat# ab150077; RRID:AB_2630356
Mouse anti-human MICA/MICB PE	Biolegend	Cat# 320906; RRID:AB_493193
Mouse anti-human HLA-A,B,C Alexa 647	Biolegend	Cat# 311416; RRID:AB_493136
Rabbit anti-SARS-Cov2	Sino Biological	Cat# 40591-T62; RRID:AB_2893171
Mouse anti-human b-actin	Abcam	Cat# ab8226; RRID:AB_306371
Goat anti-rabbit HRP	Sino Biological	Cat# SSA003; RRID:AB_2814815
Mouse anti-human ULBP-1	R & D Systems	Cat# MAB1380; RRID:AB_2214683
Mouse anti-human CD107a	BD Biosciences	Cat# 561343; RRID:AB_10644020
Mouse anti-human CD3 BV421	BD Biosciences	Cat# 562877; RRID:AB_2737860
Mouse anti-human CD14 BV650	BD Biosciences	Cat# 563420; RRID:AB_2744286
Mouse anti-human CD16 BV496	BD Biosciences	Cat# 612945; RRID: AB_2870224
Mouse anti-human CD20 BV570	BD Biosciences	Cat# 741210; RRID:AB_2870766
Mouse anti-human CD56 BV605	BD Biosciences	Cat# 742659; RRID:AB_2740950
Mouse anti-human HLA-DR APC-H7	BD Biosciences	Cat# 561358; RRID:AB_10611876
Mouse anti-human NKG2A PE-Cy7	Beckman Coulter	Cat# B10246; RRID:AB_2687887
Mouse anti-human MIP1β FITC	BD Biosciences	Cat# 560565; RRID:AB_1645489
Mouse anti-human interferon-γ BV395	BD Biosciences	Cat# 563563; RRID:AB_2738277
Mouse anti-human TNF-α BV650	BD Biosciences	Cat# 563418; RRID:AB_2738194
anti-macaque IgG HRP	NIH NHP Reagent Program	Cat# 1b3-HRP: 0320K235/070920SC
Goat anti-Mouse HRP	Abcam	Cat# ab205719; RRID:AB_2755049
Bacterial and virus strains		
SARS-CoV-2 B.1.617.2 (Delta variant)	BEI Resource	N/A
Biological samples		
NK cells (*Macaca fascicularis*)	BIDMC	N/A
Bronchoalveolar lavage from Non-Human Primates	Bioqual, Inc.	N/A
Nasal swabs from Non-Human Primates	Bioqual, Inc.	N/A
EDTA, SST, Paxgene collection tubes with whole blood, from Non-Human Primates	Bioqual, Inc.	N/A
Formalin fixed paraffin embedded skin sections excised from the left flank of C57BL/6J mice	Propath UK	N/A
Chemicals, peptides, and recombinant proteins		
Cas9 protein	IDT	Cat# 1081066
VEG-F protein	Peprotech	Cat# 100-20
Leukocyte activation cocktail	BD Biosciences	Cat# 550583
Vitronectin	StemCell Technologies	Cat# 100-0763
G418	Sigma-Aldrich	Cat# 4727878001
Puromycin	Sigma-Aldrich	Cat# P9620
Accutase	StemCell Technologies	Cat# 07920_C
CryoStor-CS10	StemCell Technologies	Cat# 07930_C

(Continued on next page)

Continued

REAGENT or RESOURCE	SOURCE	IDENTIFIER
Proteinase K	Promega	Cat# MC5005
GoTaq G2 PCR master mix	Promega	Cat# M7422
Human Heat Inactivated AB Serum	Sigma	Cat# H3667
RIPA buffer	ThermoFisher	Cat# 89900
LDS Sample Buffer	ThermoFisher	Cat# NP0007
Mini-PROTEAN TGX Gel 4–15%	Bio-Rad	Cat# 4561083
Cell Extraction Buffer	Invitrogen	Cat# FNN0011
Protease inhibitor cocktail	Sigma	Cat# P8340
Crystal Violet	Thermo Scientific	Cat# 212121000
Calcein acetoxymethyl ester CAM	Invitrogen	Cat# C3099
Critical commercial assays		
QIAquick PCR Purification Kit	Qiagen	Cat# 28104
GoTaq G2 PCR mastermix	Promega	Cat# M7823
BD Cytofix/Cytoperm Fixation Kit	ThermoFisher	Cat# AB_2869008
Live/Dead Fixable Dead Cell Stains	Invitrogen	Cat# L23101
ReliaPrep RNA miniprep	Promega	Cat# Z6010
High-Capacity cDNA Reverse Transcription Kit	Applied Biosystems	Cat# 4368814
Brilliant III Ultra-Fast SYBR green qPCR mix	Agilent Technologies	Cat# 600882
Covid-19 S-protein ELISA kit	Abcam	Cat# ab284402
FITC Annexin V Apoptosis Kit with 7-AAD	Biolegend	Cat# 640922
Cell Trace Yellow	Molecular Probes	Cat#
CD3 cell depletion kit	Miltenyi Biotech	Cat# 130-050-101
Primary cell 4D nucleofector kit	Lonza	Cat# V4XP-3024
Superscript III VILO	Invitrogen	Cat# 11754050
KPL TMB SureBlue Start solution	SeraCare	Cat# 5120-0075
KPL TMB Stop solution	SeraCare	Cat# 5150-0022
Steady-Glo Luciferase Assay	Promega	Cat# E2510
Pierce BCA Assay	ThermoFisher	Cat# 23225
AmpliCap-Max T7 High Yield Message Maker Kit	Cellscript	Cat# C-ACM04037
Super-Signal West Femto kit	ThermoFisher	Cat# 34094
Experimental models: Cell lines		
Human induced pluripotent stem cells	Thermo Fisher	Cat# A18945
HEK293T	ATCC	Cat# CRL-1573
HEK293T-hACE2	Chandrashekar et al.[64]	N/A
K562	ATCC	Cat# CCL-243
Experimental models: Organisms/strains		
C57BL/6J immunocompetent wildtype mice	Charles River Laboratories	N/A
Macaca mulatta	Bioqual, Rockville, MD	N/A
Macaca fascicularis	Bioqual, Rockville, MD	N/A
Oligonucleotides		
Human PPP1R12C (AAVS1) sgRNA: GTCACCAATCCTGTCCCTAG	This paper	N/A
Human ROSAβgeo26 sgRNA: AAGTAATTAGGACTCACTCA	This paper	N/A
Human B2M sgRNA: AAGTCAACTTCAATGTCGGA	This paper	N/A
q-PCR primers for measurement of human stemness genes	See Table S1 for oligonucleotide sequence	N/A

(Continued on next page)

Continued

REAGENT or RESOURCE	SOURCE	IDENTIFIER
Recombinant DNA		
human MICA expressing plasmid	This paper	N/A
human MICB expressing plasmid	This paper	N/A
human ULBP1 expressing plasmid	This paper	N/A
SARS-CoV-2 WA1/2020 spike gene targeting vector	This paper	N/A
psPAX2	AIDS Resource and Reagent Program	Cat# 11348
pLenti-CMV Puro-Luc	Addgene	Cat# 17477
pcDNA3.1-SARS CoV-2 SΔCT	Chandrashekar et al.[64]	N/A
Software and algorithms		
FlowJo 10	BD Biosciences	https://www.flowjo.com/solutions/flowjo
Synthego ICE tool	Synthego	https://ice.synthego.com/
GraphPad Prism	GraphPad Software	https://www.graphpad.com/scientific-software/prism/
BioRender	BioRender	https://biorender.com/
Other		
RNA Standard: SARS-CoV-2 E gene subgenomic RNA (sgRNA)	Chandrashekar et al.[64]	N/A

RESOURCE AVAILABILITY

Lead contact
Further information and requests for resources and reagents should be directed to and will be fulfilled by the corresponding author, Dr. Dan H. Barouch (dbarouch@bidmc.harvard.edu).

Materials availability
The genetically modified iPS cells (UVC) generated in this study will be made available on request, but we may require a payment and/or a completed Materials Transfer Agreement if there is potential for commercial application.

Data and code availability
- All data reported in this paper will be shared by the lead contact upon request.
- This paper does not report original code.
- Any additional information required to reanalyze the data reported in this work paper is available from the lead contact upon request.

EXPERIMENTAL MODEL AND SUBJECT DETAILS

Cell lines
Human iPS cells (Thermo Fisher) were cultured on vitronectin-coated T225cm^2 flasks using complete mTesSR Plus medium (StemCell Technologies) supplemented with 1% penicillin/streptomycin, Rock inhibitor (StemCell Technologies) at 1:1000 dilution. For drug selection, G148 was used at 500ug/mL and puromycin at 5ug/mL (Sigma-Aldrich). Cultures were maintained at 37°C, 5% CO2 in a humidified incubator. NK cell effectors were enriched from normal cynomolgus macaque (*Macaca fascicularis*, male and female) blood samples using a CD3 depletion Kit (Miltenyi Biotec). NK cells were maintained in RPMI 1640 with Glutamax (Life Technologies) supplemented with 10% heat-inactivated FCS, 2 mM, l-glutamine, 100 U/mL penicillin, 100 μg/mL streptomycin and 100 IU/mL of IL-2 and 10 ng/mL of IL-15.

Animals and study design
8- to 9-week-old female C57BL/6J immunocompetent wildtype mice (Charles River Laboratories) were randomly allocated to groups, housed at Crown Bioscience UK and acclimatized for 7-day. Irradiated or non-irradiated UVC were resuspended at 1×10^6 in 200 μL of PBS and injected subcutaneously into the left hind flank (10 animals per group). Animals were checked and weighed daily and measured for tumor growth 3 times a week in 2-dimensions using electronic calipers. Animals were sacrificed at 6 weeks and tissue surrounding the injection site was excised and prepared for histological analysis. Animal welfare for this study complies with the UK Animals Scientific Procedures Act 1986 (ASPA).

Outbred adult male and female rhesus macaques (*M. mulatta*) and cynomolgus macaques (*M. fascicularis*), 6–12 years old, were randomly allocated to groups. All macaques were housed at Bioqual. Macaques were treated with irradiated UVC at doses of either 1×10^7 or 1×10^8 cells (n = 3–6), and sham controls (n = 3–6). Prior to immunization, the cryopreserved doses of irradiated UVC were thawed at 37°C, then 900 μL of 1xPBS was added to each vial of 100 μL UVC in CryoStore freezing media. Macaques received a prime immunization of 1mL of UVC by the intramuscular route without adjuvant at week 0. At weeks 4 or 6, macaques received a boost immunization of either 1×10^7 or 1×10^8 UVC. At week 10 all macaques were challenged with 1.0×10^5 TCID$_{50}$ (1.2×10^8 RNA copies, 1.1×10^4 PFU) SARS-CoV-2, which was derived from B.1.617.2 (Delta). Viral particle titers were assessed by RT–PCR. Virus was administered as 1 mL by the intranasal route (0.5 mL in each nare) and 1 mL by the intratracheal route. All immunological and virological assays were performed blinded. All animal studies were conducted in compliance with all relevant local, state, and federal regulations and were approved by the Bioqual Institutional Animal Care and Use Committee (IACUC).

METHOD DETAILS

iPS cell irradiation and cryopreservation
Harvesting of engineered UVC was performed using accutase (StemCell Technologies) and cells were counted using a CellDrop cell counter (De-Novix). Cells were irradiated at a total single dose of 10 Gy, before centrifugation at 300 xg for 10 min followed by resuspension in 100 μL of CryoStor-CS10 freezing media (StemCell Technologies). The UVC preparations for use in non-human primate studies were analyzed for endotoxin levels (Wickham Laboratories Ltd) and absence of mycoplasma (Mycoplasma Experience Ltd).

CRISPR genetic engineering
CRISPR sgRNAs targeting the human B2M gene, PPP1R12C (AAVS1), and the ROSAβgeo26 locus were designed and validated for indel formation at the selected genomic site. Up to 6 sgRNAs per target gene were tested and the most efficient sgRNA was selected containing 2′-*O*-methyl and 3′ phosphorothioate modifications to the first three 5′ and the last three 3′ nucleotides (Synthego). 2×10^6 UVC cells were electroporated using a Neon Nucleofector (Lonza) in Buffer P3 (Lonza) with Cas9 protein (IDT) precomplexed with sgRNA, in a total volume of 100 μL using electroporation program CM138. Gene targeting vectors carrying an expression cassette for expression of human MICA or the SARS-CoV-2 WA1/2020 spike gene, targeting the Rosa26 and AAVS1 locus respectively, were co-electroporated at 4 μg. Indels introduced by CRISPR editing were detected by PCR and Sanger sequence using DNA primers designed to amplify a 600–900 base pair region surrounding the sgRNA target site. A minimum of 24 h after electroporation, genomic DNA was extracted using the DirectPCR Lysis solution (Viagen Biotech) containing Proteinase K and target regions were amplified by PCR using the GoTaq G2 PCR mastermix (Promega). Correct and unique amplification of the target regions was verified by agarose gel electrophoresis before purifying PCR products using the QIAquick PCR Purification Kit (Qiagen). For analysis by TIDE, PCR amplicons were Sanger sequenced (Eurofins or Genewiz) and paired.ab1 files of control versus edited samples were analyzed using Synthego's ICE tool (https://ice.synthego.com/).

Intracellular spike protein staining
Engineered UVC were harvested and then fixed and permeabilized using Cytofix/Cytoperm Fixation/Permeabilization Solution (ThermoFisher). Cells were then stained for intracellular spike protein using an Anti-SARS-CoV-2 Spike Glycoprotein S1 antibody (Abcam, ab275759, 1:50) followed by Goat Anti-Rabbit IgG H&L (Alexa Fluor 488) (Abcam, ab150077, 1:500). Flow analysis was carried out on a Fortessa flow cytometer (BD Bioscience), and data analyzed, and flow cytometry figures generated using FlowJo 10 software (BD Biosciences).

Flow cytometry analysis of cell surface antigen expression
For flow cytometric analysis of cell surface expression of MHC-I, MICA and SARS-CoV-2 spike protein, cells were harvested from culture plates and washed using PBS with 1% Bovine Serum Albumen (Thermo Scientific) and were then stained with PE anti-human MICA/MICB Antibody (6D4, Biolegend), Alexa Fluor 647 anti-human HLA-A,B,C (W6/32, Biolegend), and anti-SARS-CoV-2 Spike Glycoprotein S1 antibody (Abcam, ab275759, 1:50) followed by Goat Anti-Rabbit IgG H&L (Alexa Fluor 488) (Abcam, ab150077, 1:500). Live/Dead Fixable Dead Cell Stains (Invitrogen) were included in all experiments to exclude dead cells. After staining, cells were resuspended in PBS with 2% Human Heat Inactivated AB Serum (Sigma) and 0.1 M EDTA pH 8.0 (Invitrogen) before analysis on a Fortessa flow cytometer (BD Bioscience) and data analyzed using FlowJo 10 software (BD Biosciences).

Western blot
The SARS-CoV-2 spike glycoprotein was detected in UVC lysates by western blotting. Briefly, cells were lysed by RIPA buffer (20 mM Tris-HCl pH 7.5, 150 mM NaCl, 1 mM EDTA, 0.1% SDS, 1% NP40, 1x protease inhibitor cocktail). Samples were spun at 4°C for 10 min at 12,000 xg and the pellet discarded. Protein content was measured using BCA Assay (ThermoFisher) using a PHERAstar plate reader (BMG Labtech) at 560 nm. LDS Sample Buffer was added to 30 ng of protein sample to make a 1x solution, with 0.5 μL of b-mercaptoethanol per well and heated at 70°C for 10 min before separation on a polyacrylamide gel (Bio-Rad Mini-PRO-TEAN TGX Gel 4–15%) and transferred to a PVDF membrane. Membranes were blocked in blocking buffer (5% non-fat powdered

milk in TBST), before incubation with primary antibodies in blocking buffer (Rabbit polyclonal anti-SARS-Cov2, Sino Biological 40,591-T62, 1:6000 dilution or Mouse b-actin, Abcam 8226, 1 μg/mL), detected with HRP conjugated secondaries in blocking buffer (Goat anti-Rabbit HRP, Sino Biological SSA003, 0.5 μg/mL or Goat anti-Mouse HRP, Abcam ab205719, 1: 4000 dilution) and visualised using the Super-Signal West Femto kit (ThermoFisher) as per kit instructions.

qPCR measurement of stem cell factors

Total RNA was extracted from UVC cells using the ReliaPrep RNA miniprep (Promega) according to the manufacturer's instructions (a DNase treatment was included for all samples), and RNA concentration and absorbance ratios were measured using a Nanodrop One Spectrophotometer (ThermoFisher). cDNA was synthesized using a High-Capacity cDNA Reverse Transcription Kit (the Applied Biosystems) in a total volume of 20 μL to produce DNA that was subsequently assessed by spectrophotometric analysis and diluted to 100 ng/μL. Individual master mixes with each of the DNA-primer combinations for detection of human SOX2, NANOG, OCT4, DCN, Vimentin, HES5 and GATA6 genes were made for 3 replicates using the Brilliant III Ultra-Fast SYBR green qPCR master mix (Agilent Technologies) and analyzed on a CFX Opus Real-Time PCR system (BioRad) using the following program: 95°C for 15 min for 1 cycle; 95°C for 15 s for 40 cycles; 60°C for 30 s.

SARS-CoV-2 spike protein ELISA

Cell pellets were harvested and lysed in 20 μL Cell Extraction Buffer (Invitrogen) containing protease inhibitors (Sigma) on ice for 30 min, with 3 brief vortexing every 10 min. Samples were centrifuged at 13,000 rpm for 10 min at 4°C to pellet insoluble contents. S1 Spike protein was detected using a Covid-19 S-protein ELISA kit (Abcam) specific to S1RBD. Samples were diluted to a range determined to be within the working range of the ELISA kit used and the assay procedure was followed as per manufacturer's instructions. The resulting colorimetric signal was detected at 450 nm using a PHERAstar (BMG LABTECH) plate reader. GraphPad Prism was used to plot a standard curve and interpolate the sample values using a 4-parameter logistic fit.

UVC proliferation and apoptosis assays

To quantify apoptosis of UVC post-irradiation, cells were stained using a FITC Annexin V Apoptosis Detection Kit with 7-AAD (Biolegend). Proliferation of cells was measured by staining of control and Irradiated UVC with 2 μM Cell Trace Yellow (Invitrogen) according to kit protocol and analyzing the dilution of the dye at 24-h periods over 3-days and measuring fluorescence intensity. Flow analysis was carried out on a Fortessa flow cytometer (BD Bioscience), and data analyzed, and flow cytometry figures generated using FlowJo 10 software (BD Biosciences).

Colony formation assay

Cells were seeded in vitronectin coated 60 mm diameter plastic culture dishes in triplicate, at densities of between 100 and 3000 cells per dish, and cultured in mTeSR-Plus with Rock Inhibitor (StemCell Technologies) for 24 h to allow cells to adhere. Media was then replaced with mTeSR-Plus without Rock Inhibitor for an additional 9 days. Media was replaced every 2 days before finally being removed and plates dried and stained with 0.25% Crystal Violet (Thermo Scientific) in 20% methanol to visualise colonies prior to counting.

CAM cytotoxicity assay

Both MHC-I expressing and MHC-I deficient (B2M knockout) UVC were used as target cells for NK cell cytotoxicity assay. Trypsinized cells were stained with calcein acetoxymethyl ester (CAM, Invitrogen) at a 10 μM concentration for 1 h at 37°C and then washed to remove excess dye. NK cells highly enriched from normal cynomolgus macaque (*Macaca fascicularis*) blood samples using a CD3 depletion kit (Miltenyi Biotec), were used as effector cells. NK cell effectors and stained target cells were co-cultured in 96 well round bottom plates at effector: target (E:T) ratios of 1:1 and 5:1. Control wells included – only target cells for spontaneous release of CAM and target cells treated with Triton X-100 for maximum release of CAM. At the end of 4-h incubation, supernatant was collected for CAM measurement in a fluorescent plate reader at 530 nm. Percent-specific lysis = (test release - spontaneous release)/(maximum release - spontaneous release).

Nucleofection of NKG2D ligands in iPS cells

UVC were cultured in EGM2 (Lonza) media supplemented with 20 ng/mL VEG-F (Peprotech) until 70–90% confluent, in tissue culture flasks pre-coated with sterile 0.1% gelatin in PBS for 1 h at 37°C. The cells were removed from culture flasks using trypsin, washed, and transfected with plasmid DNA containing either MICA, MICB or ULBP-1 genes after optimizing nucleofection conditions using primary cell 4D nucleofector kit and 4D nucleofector system (Lonza). After 48 h of culture, transfected cells were stained with aqua dye for live/dead discrimination and corresponding antibodies- MICA/MICB (Clone 6D4, PE, BioLegend) or ULBP-1 (clone 170,818, PE, R & D Systems). Stained cells were fixed with 2% paraformaldehyde and acquired on LSRII flow cytometer. Transfection efficiency was calculated as % live cells expressing transfected protein.

NK cell intracellular cytokine staining assay

UVC target and NK effector cells were plated at E:T ratio of 2:1 in a 96 well round bottom plate. Anti-CD107a antibody (clone H4A3, ECD conjugate, BD Biosciences), brefeldin A and monensin (BD Biosciences) were added to all the samples prior to incubation. After

6 h of incubation at 37°C, the cells were washed and stained with aqua dye used for live and dead cell discrimination for 20 min at room temperature. The cells were then washed and stained for surface markers that included CD3 (SP34.2, BV421, BD Biosciences), CD14 (M5E2, BV650, BD Biosciences), CD16 (3G8, BUV496, BD Biosciences), CD20 (L27, BV570, BD Biosciences), CD56 (NCAM1.2, BV605, BD Biosciences), HLA-DR (G46-6, APC-H7, BD Biosciences) and NKG2A (Z199, PE-Cy7, Beckman Coulter) to delineate NK effector cells. Following incubation for 20 min, cells were washed and permeabilized using fix & perm reagent (Thermofisher Scientific) as per manufacturer's recommendation. Intracellular cytokine staining was performed for macrophage inflammatory protein 1β (MIP-1β; D21-1351, FITC, BD Biosciences) interferon-γ (IFN-γ; B27, BUV395, BD Biosciences), tumor necrosis factor alpha (TNF-α; Mab11, BV650, BD Biosciences) at 4°C for 15 min. Cells were washed, fixed, and acquired on LSRII flow cytometer. Unstimulated NK cells were used for background subtraction of percent positive cells. NK cells stimulated with leukocyte activation cocktail (BD Biosciences) were used as positive control for the assay.

Immunohistochemical analysis

Following fixation in 10% NBF, tissue samples excised from mice injected with UVC were dehydrated in graded alcohols and embedded side-on in paraffin wax. FFPE blocks were trimmed until at full-face before placing on slides for H&E staining. Following heat fixation to the slide, the tissue sections were deparaffinised in xylene and rehydrated through graded alcohol before staining with Haematoxylin and Eosin. Whole slide scans were imaged using a Hamamatsu slide scanner.

Subgenomic viral mRNA assay

SARS-CoV-2 *E* gene sgRNA was assessed by RT–PCR using primers and probes as previously described.[49–52] In brief, to generate a standard curve, the SARS-CoV-2 *E* gene sgRNA was cloned into a pcDNA3.1 expression plasmid; this insert was transcribed using an AmpliCap-Max T7 High Yield Message Maker Kit (Cellscript) to obtain RNA for standards. Before RT–PCR, samples collected from challenged macaques or standards were reverse-transcribed using Superscript III VILO (Invitrogen) according to the manufacturer's instructions. A Taqman custom gene expression assay (ThermoFisher Scientific) was designed using the sequences targeting the *E* gene sgRNA. Reactions were carried out on a QuantStudio 6 and 7 Flex Real-Time PCR System (Applied Biosystems) according to the manufacturer's specifications. Standard curves were used to calculate sgRNA in copies per mL or per swab; the quantitative assay sensitivity was 50 copies per mL or per swab.

Serum antibody ELISA

RBD-specific binding antibodies were assessed by ELISA as previously described.[9,10] In brief, 96-well plates were coated with 1 μg mL−1 SARS-CoV-2 RBD protein (A. Schmidt, MassCPR) in 1× DPBS and incubated at 4°C overnight. After incubation, plates were washed once with wash buffer (0.05% Tween 20 in 1× DPBS) and blocked with 350 μL casein block per well for 2–3 h at room temperature. After incubation, block solution was discarded, and plates were blotted dry. Serial dilutions of heat-inactivated serum diluted in casein block were added to wells and plates were incubated for 1 h at room temperature, before three further washes and a 1-h incubation with a 1:1,000 dilution of anti-macaque IgG HRP (NIH NHP Reagent Program) at room temperature in the dark. Plates were then washed three times, and 100 μL of SeraCare KPL TMB SureBlue Start solution was added to each well; plate development was halted by the addition of 100 μL SeraCare KPL TMB Stop solution per well. The absorbance at 450 nm was recorded using a VersaMax or Omega microplate reader. ELISA endpoint titers were defined as the highest reciprocal serum dilution that yielded an absorbance >0.2. The log_{10}(endpoint titers) are reported.

Pseudovirus neutralization assay

The SARS-CoV-2 pseudovirus expressing a luciferase reporter gene were generated in a similar approach to that previously described.[9,10,16] In brief, the packaging construct psPAX2 (AIDS Resource and Reagent Program), luciferase reporter plasmid pLenti-CMV Puro-Luc (Addgene), and spike protein expressing pcDNA3.1-SARS-CoV-2 SΔCT were co-transfected into HEK293T cells with calcium phosphate. The supernatants containing the pseudotype viruses were collected 48 h after transfection; pseudotype viruses were purified by filtration with 0.45-μm filter. To determine the neutralization activity of the antisera from vaccinated macaques, HEK293T-hACE2 cells were seeded in 96-well tissue culture plates at a density of 1.75×10^4 cells per well overnight. 2-fold serial dilutions of heat-inactivated serum samples were prepared and mixed with 50 μL of pseudovirus. The mixture was incubated at 37°C for 1 h before adding to HEK293T-hACE2 cells. After 48 h, cells were lysed in Steady-Glo Luciferase Assay (Promega) according to the manufacturer's instructions. SARS-CoV-2 neutralization titers were defined as the sample dilution at which a 50% reduction in relative light units was observed relative to the average of the virus control wells.

QUANTIFICATION AND STATISTICAL ANALYSIS

Statistical differences between two sample groups, where appropriate, were analyzed by a standard Student's two-tailed, non-paired, t-test and between three or more sample groups using two-way or three-way ANOVA using GraphPad Prism 9. Analysis of virological data was performed using two-sided Mann–Whitney tests. Correlations were assessed by two-sided Spearman rank-correlation tests. p values are included in the figures or referred to in the legends where statistical analyses have been carried out. p values of less than 0.05 were considered significant.